Eur. Phys. J. D **20**, 251–260 (2002)
DOI: 10.1140/epjd/e2002-00130-3

THE EUROPEAN PHYSICAL JOURNAL D

Optical properties of silver clusters formed by ion irradiation

J.C. Pivin[1,a], M.A. García[2], H. Hofmeister[3], A. Martucci[4], M. Sendova Vassileva[5], M. Nikolaeva[5], O. Kaitasov[1], and J. Llopis[2]

[1] Centre de Spectrométrie Nucléaire et de Spectrométrie de Masse, bâtiment 108, 91405 Orsay Campus, France
[2] Departamento de Física de Materiales, Facultad de Ciencias Físicas, Universidad Complutense de Madrid, 28040 Madrid, Spain
[3] Max-Planck-Institut für Mikrostrukturphysik, Weinberg 2, 06120 Halle, Germany
[4] Dipartimento di Ingegneria Meccanica, Universita di Padova, via Marzolo 9, 35131 Padova, Italy
[5] Central Laboratory for Solar Energy and New Energy Sources, Bulgarian Academy of Sciences, 72 Tzarigradsko Chaussee blvd., 1784 Sofia, Bulgaria

Received 10 January 2002 / Received in final form 26 April 2002
Published online 19 July 2002 –

Abstract. Precipitation of silver clusters in silica is achieved by different methods: ion implantation, ion beam mixing of superimposed layers and ion irradiation of films deposited by means of co-sputtering or sol-gel technique. Main features of the nanoparticles depending on the preparation method are investigated by TEM. The optical extinction resonance of these clusters is analysed in terms of sizes and interaction between the clusters on the basis of calculations. We found that resonances in sputtered and gel films with low metal concentrations are well described by plasmon polaritons in isolated clusters and calculations based on Mie theory allow the study of their growth under irradiation. This theory is not appropriate to describe the optical response of silver clusters in silica implanted with Ag concentrations higher than 5 at.% or in ion beam mixed films, because of the interaction between clusters. Using an effective medium model, it is demonstrated that the random dispersion of clusters in implantation films causes fluctuations and, on average, an increase of the clusters polarization. On the contrary, the particular arrangement of the clusters with a bimodal size distribution in ion beam mixed films induces a screening effect between the clusters of largest size.

PACS. 61.46.+w Nanoscale materials: clusters, nanoparticles, nanotubes, and nanocrystals – 78.40.-q Absorption and reflection spectra: visible and ultraviolet

1 Introduction

Noble metals have been implanted in insulators for many years with the purpose of obtaining metallic clusters with high filling factors close to the surface, expecting that these implantation films exhibit a stronger non-linearity of refractive index than colloid films synthesized by other processes [1]. However, the potential applications of high-dose implantation films are limited by their cost and the inhomogeneity in size and depth distribution of the metal clusters. Recently, ion beam mixing of oxide/metal/oxide superimposed layers has been proposed as an alternative method to achieve the same purpose, with ion fluences an order of magnitude lower [2]. In the case of noble metals, the result of irradiation is not a real mixing, due to their insolubility in most of the oxides considered (SiO_2, Al_2O_3, TiO_2, ZrO_2), but a lateral diffusion of the metal atoms to form spheroidal clusters of sizes 2–3 times the metal layer thickness. However, Rutherford backscattering spectra (RBS) and TEM images recorded after irradiation with increasing ion fluences evidence that the metal atoms ejected from these large clusters by collisions diffuse over significant distances with respect to the cascade dimension before precipitating again. The new clusters formed by this mixing-unmixing process are very small (∼1 nm), arranged in a concentric halo around the central cluster and their number increases in proportion to the ion fluence, Φ as the number of displaced atoms [2]. On the other hand, the ion irradiation of other types of films, with a well defined interface to the substrate and an appropriate refractive index, is more suitable than implantation or mixing for fabricating wave-guides. Examples presented here are the irradiation of co-sputtered SiO_2:Ag films in non-equilibrium solid solution as well as gel films containing Ag introduced by adding a salt to the precursor.

It is well-known that clusters of free-electron metals in dielectric matrices exhibit optical absorption bands in the visible ascribed to their surface plasmon resonances [3].

[a] e-mail: pivin@csnsm.in2p3.fr

The main features of these bands are related to the matrix refractive index and to the characteristics of the clusters: size, shape and spatial distribution. Therefore, several models have been developed to connect the optical absorption spectra with the properties of the clusters. Among them, Mie theory [3] permits to calculate the mean energy and shape of the resonance as a function of the matrix and cluster size, provided that clusters are spherical and isolated (*i.e.* interacting effects may be neglected). The effect of other parameters, as the cluster shape and the clusters interaction, may be analyzed by means of an effective medium theory presented here.

The purpose of present paper is to correlate the modifications of absorption resonances as a function of the ion fluence in films prepared by the previously described methods with the microstructural changes induced by the irradiation. We discuss if the analysis of absorption bands allows a quantitative assessment of the cluster growth. Effects of the electromagnetic interaction between clusters in films with high volume fractions of metallic phase are also investigated. The validity of those calculations is analyzed for the different types of structure, stating the parameters that mainly governs the shape of optical absorption spectra.

2 Experiments and calculations

2.1 Preparation of films and irradiation

Implantations of 10^{16}, 2×10^{16}, 5×10^{16} and 10^{17} ions/cm^2 were performed in silica (Herasil grade) at an energy of 150 keV. The ion current was limited to 0.3 μA cm^{-2} and the sample holder cooled with water in order to prevent a target heating over 20 °C (also applied for other irradiations). RBS analyses of these samples demonstrated a Gaussian distribution of Ag concentration, peaking at a depth of 76 nm and having a width of 19 nm, for the fluences of 1 to 5×10^{16} (concentrations of 3, 6, 15%) in agreement with TRIM calculations [4]. No significant sputtering occurred for the highest fluence, but the Ag concentration, 28%, was more homogeneous in the outer 40 nm of the implanted layer.

Samples for ion beam mixing experiments were prepared by successive deposition of Ag and SiO_2 layers, using electron-gun evaporation, onto silica substrates at high vacuum of 10^{-5} Pa base pressure. They were irradiated with incremented fluences of 4.5 MeV Au ions, easily delivered by the used accelerator and producing as many collisions as ionizations over their path of about 1 μm: densities of energy transferred to nuclei and electrons are comparable and of the order of 300 eV/10^{15} atoms/ion/cm^2 [4]. We studied single metal layers, buried beneath 100 nm SiO_2, instead of multilayers with a more homogeneous depth distribution of clusters, because this enabled us to correlate the modifications of optical transmittance with the known mixing kinetics in this type of specimens [2]. Spectra from a 8 nm thick Ag layer have been chosen here as an example.

SiO_2:Ag films with homogeneous Ag atomic concentrations of 0.5 to 2.5% were deposited by co-sputtering under an Ar pressure of 0.5 Pa. It is worth to note that the stoichiometry of the oxide matrix found by means of RBS and nuclear reaction analysis is $Si_{0.31}O_{0.69}$. Indeed, a depletion in oxygen concentration favors the Ag precipitation before any treatment [5] and a precipitation was already observed in presently studied films. The thickness of films for transmittance measurements was 750 nm. Some of the samples were annealed, for 1 h at temperatures ranging from 500 to 900 °C in vacuum, for a purpose of cluster sizes comparison.

Tetraethoxysilane (TEOS) and silver fluoroborate mixed in solution were used to synthesize silica gels with 0.1 to 1.5 at.% Ag in solution. The solutions were spun at a speed of 3 000 rpm on silica wafers for obtaining films with a thickness of the order of 500 nm (maximum thickness for good adhesion). RBS analyses of these films put into evidence depth gradients of Ag concentration, generally with maxima at the interfaces and a plateau in the bulk of the film. This inhomogeneity is typical of noble metals in gel films [6].

Plane-view and cross-sectional TEM imaging was used to study the variations of size and density of clusters as a function of the ion fluence Φ. The deposition of co-sputtered and gel films thinner than for optical measurements, on rock salt or silicon, simplifies the preparation process for plane-view imaging, since it is sufficient to dissolve the substrate in water or a solution of 10% HF in water, and improves the statistics in measurements of cluster size. Nevertheless, the gradients of Ag concentration in the vicinity of the substrate interfaces in gels and the preferential nucleation of Ag clusters on defects (voids, scratches) [5] make them less reliable.

Measurements of optical transmittance were made from 200 to 800 nm using a Cary UV-VIS-NIR dual beam spectrometer.

2.2 Calculations

Two types of calculations, based on Mie theory and on a effective medium model were used, depending on the filling factor, geometry and spatial distribution of clusters. The Mie theory [3], allows to calculate the exact optical response of the system by solving the Maxwell equations in the medium, provided that the clusters are spherical and isolated from each other. A detailed description of this theory may be found in reference [3]. Here we summarize some results of these calculations for clusters of increasing size, to avoid digressions in the following discussion. In the case of Ag, clusters behave as electric dipoles when their radii R are below 40 nm. Absorption by multipoles of higher order and scattering do not contribute to the optical extinction. Within this "quasi-static" regime of resonance, the extinction cross-section σ_{ext} of a single cluster (which in this case is identical to the absorption

cross-section) approximates to:

$$\sigma_{\rm ext}(R,\omega) = \frac{9\omega}{c}\varepsilon_{\rm m}^{3/2}\,\frac{4\pi R^3}{3}\,\frac{{\rm Im}(\varepsilon)}{\left[{\rm Re}(\varepsilon)+2{\rm Re}(\varepsilon_{\rm m})\right]^2+{\rm Im}(\varepsilon)^2} \tag{1}$$

where ω is the angular frequency of incident light, c the speed of light in vacuum, ε is the complex dielectric function of the metal, $\varepsilon_{\rm m}$ that of the matrix, Re and Im their real and imaginary parts. In the case of Ag, the integral of the σ function over the energy range of the plasmon resonance increases linearly with R^3 up to sizes of about 10 nm whereas it decreases by a factor 2 for sizes in the range 10 to 30 nm (this point is often disregarded in calculations of the optical density). Consequently, for a set of clusters smaller than 10 nm, changes in the volume fraction of metallic phase caused by thermal or irradiation treatment can be assessed unambiguously by measurements of the optical density. Moreover, the relevant dimension to be averaged for plasmon resonances in films with a distribution of cluster sizes is not the radius of clusters but their volume.

When the interaction between clusters cannot be neglected, because of the high filling factor (as it is generally the case in ion implanted and ion beam mixed layers) it is necessary to apply an effective medium theory, which substitutes the inhomogeneous matrix-cluster system with a homogeneous medium (with an "effective dielectric function") that has the same optical response. Application of this type of theory presumes that the problem of the interaction between each cluster and the incident electric field can be simplified by considering that the cluster behaves as a dipole (this is true for all the presently studied systems according to the results of Mie calculations reported above). Although the effective medium theories are not so exact as the Mie theory, their calculations are much easier, and therefore it is possible to take into account other factors affecting the mean energy and width of resonance peaks: the shape of clusters which are not necessarily spherical, their interaction depending on the spatial arrangement and the filling factor. In the model presently used [7], the fundamental expression of electrodynamics for the polarizability α of clusters is modified by introducing in the latter expression a parameter β to account for the dependence of α on the cluster shape:

$$\alpha = \frac{V(\varepsilon-\varepsilon_{\rm m})}{\varepsilon_{\rm m}+\beta(\varepsilon-\varepsilon_{\rm m})} \tag{2}$$

where V is the cluster volume. The value of β is equal to 1/3 for a cluster with a spherical shape. As for the Mie calculations performed in this study, the dielectric function of small metal clusters is corrected for the variation of the electron mean free path with the radius R, according to the formula proposed by Hövel *et al.* [8]:

$$\varepsilon(\omega,R) = \varepsilon_{\rm bulk}(\omega) + \frac{\omega_{\rm p}^2}{\omega^2+{\rm i}\omega\gamma_0} - \frac{\omega_{\rm p}^2}{\omega^2+{\rm i}\omega(\gamma_0+Av_{\rm F}/R)} \tag{3}$$

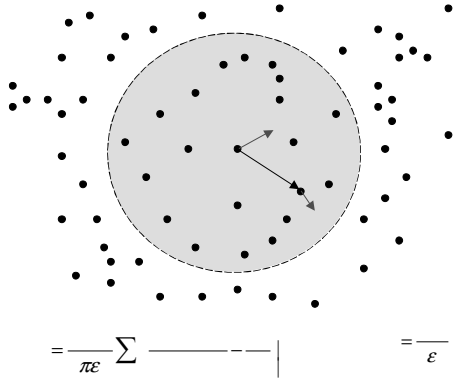

Fig. 1. The electric field acting on a particle i is calculated using an imaginary sphere to cut the space in two parts. The electric field $\mathbf{E}_{\rm close}$ created by close clusters (inside the sphere) depends on their spatial distribution, whereas for the other clusters, the field $\mathbf{E}_{\rm remote}$ is $\mathbf{P}/3\varepsilon_{\rm m}$. The local field is the sum of $\mathbf{E}_{\rm ext}+\mathbf{E}_{\rm close}+\mathbf{E}_{\rm remote}$.

$\omega_{\rm p}$, $v_{\rm F}$ and γ_0 being the plasmon frequency, the Fermi velocity and the relaxation frequency (or damping constant) of the bulk metal respectively and A a phenomenological parameter including details of the scattering process. Experimentally, the value of A is 1 for silica glasses and ceramics [8].

The local field at a certain cluster position, $\mathbf{E}_{\rm loc}$, is the sum of the external applied field $\mathbf{E}_{\rm ext}$, plus that created by the rest of the clusters. The latter may be calculated by using the Lorentz formalism, as shown in Figure 1. The polarization $\mathbf{P}$ of the considered cluster by the effective medium is parallel to the direction x of the applied field $\mathbf{E}_{\rm ext}$ and no preferential orientation of the individual dipoles is expected in the y or z-directions. Thus, like $\mathbf{E}_{\rm ext}$, $\mathbf{E}_{\rm loc}$ is also in the x-direction and its magnitude is given by:

$$E_{\rm loc} = E_{\rm ext} + \frac{P}{3\varepsilon_{\rm m}} + \frac{1}{4\pi\varepsilon_{\rm m}}\sum_j\left[\frac{3x_{ij}^2\,p_{jx}}{r_{ij}^5} - \frac{p_{jx}}{r_{ij}^3}\right] \tag{4}$$

as $p_{jy}\,y_{ij}+p_{jz}z_{ij}\approx 0$ when the summation is extended to a large number of clusters. We define here the parameter K as:

$$K = \sum_j\left[\frac{3x_{ij}^2}{r_{ij}^5} - \frac{1}{r_{ij}^3}\right]\frac{p_{jx}}{P} \tag{5}$$

$3K/4\pi$ is the ratio of the contribution to the local electric field of close clusters, with dipolar moments $\mathbf{p}_j$ and at distance r_{ij} of the considered cluster i, to that of clusters outside the Lorentz sphere (Fig. 1). As the former is largely dependent of the spatial distribution of the clusters, whereas the latter is almost independent, the parameter K describes the effect of the local arrangement on the interaction between the clusters. Replacing K in equation (4), we obtain for the polarization of a set of

clusters with a number density N:

$$P = N\,\alpha\,E_{\rm loc} = \frac{N\,\alpha\,E_{\rm ext}}{1 - N\alpha\left(\frac{1}{3\varepsilon_{\rm m}} + \frac{K}{4\pi\varepsilon_{\rm m}}\right)}\cdot \qquad (6)$$

When the clusters are regularly spaced on a cubic lattice the value of K is zero and the degree of polarization is determined by the filling factor $f = NV$.

Assuming that the matrix-clusters system behaves as an effective medium with a complex dielectric function $\varepsilon_{\rm ef}$, the magnitude of the polarization of this medium should be $P = (\varepsilon_{\rm ef} - \varepsilon_{\rm m})E_{\rm ext}$ and hence:

$$\varepsilon_{\rm ef} = \varepsilon_{\rm m} + \frac{N\alpha}{1 - N\alpha\left(\frac{1}{3\varepsilon_{\rm m}} + \frac{K}{4\pi\varepsilon_{\rm m}}\right)}\cdot \qquad (7)$$

The absorption coefficient k of the material (optical density OD) is derived by writing $\varepsilon = (n + {\rm i}k)^2$:

$$k({\rm cm}^{-1}) = \frac{\sqrt{2}}{\hbar c}E({\rm eV})\sqrt{-{\rm Re}(\varepsilon_{\rm ef}) + \sqrt{{\rm Re}(\varepsilon_{\rm ef})^2 + {\rm Im}(\varepsilon_{\rm ef})^2}}. \qquad (8)$$

It must be noted that the calculated functions $\varepsilon_{\rm ef}(E)$ and $k(E)$ are found identical to those obtained with the Mie model for the particular case $K = 0$, $\beta = 1/3$ and filling factors f below 5%.

All simulations presented hereafter are normalised to the height of experimental spectra for 2 reasons:

(i) calculations of Mie type concern a single cluster;
(ii) the thickness of implantation and mixed films is undefined so the concept of absorption coefficient loses part of its meaning.

A constant refractive index $n_{\rm m}$ of 1.475 was used in all calculations since this value was measured by spectroscopic ellipsometry for silica and silica gel films without silver.

3 Results and discussion

3.1 Co-sputtered films

TEM images show that clusters are already present in these films before ion irradiation, because of the intrusion of the surface by the plasma [5]. Their density is generally homogeneous, but images of cross-sections put into evidence that they are aligned perpendicular to the surface, most probably at the boundaries between matrix columns which are typical of sputtered coatings [5]. Their size is very small and from TEM images only a rough estimate of about 0.3 nm or less can be given for the radius. After ion irradiation, narrow cluster size distributions are observed (see micrograph and size distribution in Fig. 2). The mean radius is found to be between 1 and 2 nm for fluences above 10^{15} ions/cm^2, depending on the Ag concentration. The sample shown in Figure 2 was chosen because it exhibited a concentration gradient from 1.0% Ag at the surface up to 2.0% close to the interface. Increases of the number density and mean size of clusters with depth are observed accordingly in the image. The number density varies by 30% between the two interfaces and the mean size increases from 1.4 ± 0.4 nm in the third part of the thickness close to the surface to 1.8 ± 0.4 nm in the vicinity of the substrate interface.

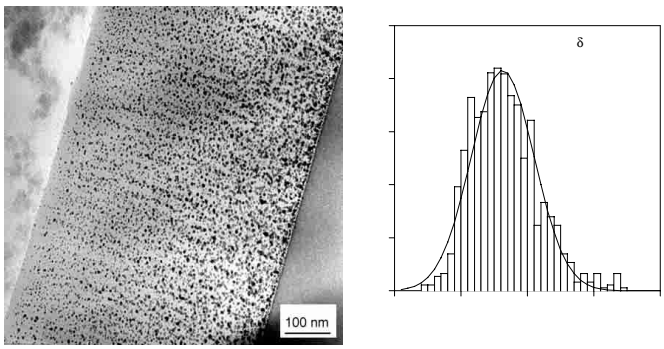

Fig. 2. (Left) TEM image of the cross-section of a co-sputtered SiO_2:Ag film with a concentration gradient of 2.0 to 1.0 at.% Ag from the interface to the surface, after irradiation with 8×10^{14} Au ions; (right) histogram of cluster sizes resulting from 1 000 measurements in the whole thickness of the film. The mean radius $\langle R\rangle$ and straggling in the distribution δR indicated in the figure are those found with a Gaussian fit of the histogram (continuous line).

Figure 3 shows optical absorption spectra of samples having a homogeneous concentration equal to the mean concentration in the sample of Figure 2. A resonance is observed even in the spectrum from the unirradiated sample. For fluences Φ below 10^{14} ions/cm^2, the peak slightly shifts towards lower energy with the increasing Φ and its shape changes very little. For larger fluences, the peak remains centred at a constant energy and becomes narrower.

The filling factor in these films is below 5%. As already stated, simulations based on the effective medium model show that, for a such a low filling factor, interaction effects can be neglected. Thus, the features of resonance peaks are mainly determined by the cluster size and shape. The resolution of the used microscope does not allow us to define the shape of the clusters, so the most simple case of spherical clusters will be assumed. Without performing calculations, one can deduce from the decrease of the peak width for Φ values above 10^{14} ions/cm^2 that the clusters grow, since the Mie theory predicts a strong decrease of this width with the increasing size up to 5 nm. In addition, the integral of the resonance peak rises at most of 10% up to the fluence of 10^{14} ions/cm^2 then remains constant and equal to that measured for films with the same Ag concentration annealed at temperatures T in the range 600 to 800 °C (a slight evaporation of Ag occurs at 900 °C), in which all Ag is undoubtedly precipitated. We conclude from this result that almost all Ag is already precipitated at low irradiation fluence, since the integral of $\sigma_{\rm ext}$ is proportional to the total volume of metallic phase when the radius of clusters is less than 10 nm, and some of the clusters grow at the expense of others.

Table 1. Values of mean radius R_1 and straggling δR_1 obtained by fitting the distribution of sizes observed in TEM for a few sputtered and gel films (equal to the value found by arithmetical averaging within 1–5%), radius R_2 obtained by averaging the volumes, uniform radius R_3 giving the same shape of resonance than the distribution and radius R_4 permitting to fit the absorption resonance recorded from a similar specimen.

specimen	SiO_2:Ag0.5%, 5×10^{14} ions	SiO_2:Ag1.0%, 5×10^{14} ions	SiO_2:Ag1.0%, 10^{15} ions	SiO_2:Ag1.5%, 8×10^{14} ions	TEOS:Ag0.3%, 2×10^{14} ions	TEOS:Ag0.3%, 1.5×10^{15} ions
$R_1 \pm \delta R_1$ (nm)	0.39 ± 0.11	1.05 ± 0.30	1.48 ± 0.48	1.60 ± 0.46	0.90 ± 0.30	1.45 ± 0.45
R_2 (nm)	0.50	1.25	1.82	1.85	1.10	1.75
R_3 (nm)	0.50	1.30	1.80	1.90	1.15	1.80
R_4 (nm)	0.45	1.05	1.50	1.50	0.90	1.40

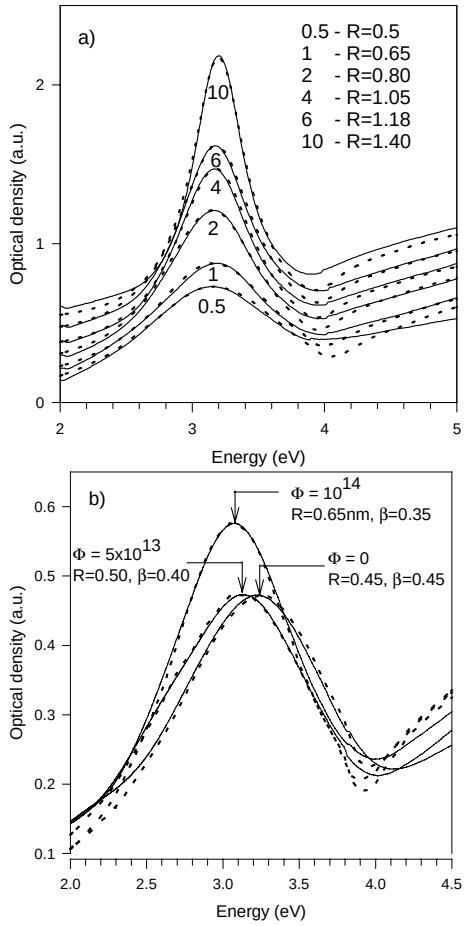

Fig. 3. (a) Optical density of Ag clusters in a co-sputtered SiO_2:Ag film containing 1.5 at.% Ag, after irradiation with fluences indicated in multiples of 10^{14} ions/cm^2 (continuous lines) and Mie simulations fitting spectra (dotted lines). Spectra are shifted vertically for the sake of clarity. (b) Optical density spectra of the same film as-deposited and irradiated with low fluences (continuous lines) and fits using the model of effective medium (dotted lines) with $f = 1.5\%$, $K = 0$, values of the radius and of the shape factor indicated in the figure.

In order to fit the experimental spectra, Mie resonances for incremented cluster sizes should be weighted by the size histogram of clusters observed in TEM. Simulations have been performed applying the few size histograms which were available and the uniform size giving the same resonance was estimated (Tab. 1). The comparison of simulations shows that assuming a uniform size R_3 leads systematically to overestimate the mean radius by about 20% with respect to the value R_1 found by arithmetical averaging of the radii or by fitting the distribution as done in Figure 2. However, the agreement between the uniform size giving the same resonance than the histogram and the radius value R_2 found by averaging the volumes is very good. Therefore, assuming a uniform size for fitting spectra should permit to assess quantitatively changes of the mean volume with the Ag concentration and ion fluence. Moreover, the determination of the size distribution corresponding to each spectrum would make little sense taking into account the uncertainties on sizes measured by TEM, due to the limited resolution and to artifacts when these measurements are performed on plane view specimens (linked to effects mentioned in Sect. 2.1).

The absorption spectra of sputtered films irradiated with ion fluences over 10^{14} ions/cm^2 are well fitted by plasmon polariton peaks of isolated clusters with spherical shape, up to the threshold of absorption by bound electrons at 3.8 eV (see Fig. 3a). The slight discrepancy between the spectra and simulations at higher energies is ascribed to the crude assumption made in equation (3) that the dielectric susceptibility, $\chi_{\text{interband}}$, of these bound electrons in small clusters is the same than in the bulk metal. When comparing the uniform size R_4 used for fitting the spectra to values of mean sizes R_1, R_2 measured by TEM, a better agreement is found with value R_1 than with the expected value R_2 (Tab. 1). This result points to an overestimation of the size of small clusters from TEM images.

According to the simulations, the mean size of clusters increases approximately as the ion fluence then levels off at a fluence increasing with the Ag concentration (see Fig. 4). Theoretically, for particles of a phase B growing by thermal diffusion in a matrix A, a linear increase of the size with time is expected when the diffusion rate of B atoms is much higher than the rate of adsorption or of desorption at the particle/matrix interfaces [11]. Let us note that, in the case of irradiation, one must distinguish the radiation-induced diffusion over short distances during collision cascades from the radiation-enhanced diffusion occurring after the ballistic process, when the created defects are mobile [12]. The mobility of Ag atoms in the silica matrix is increased in present conditions of irradiation, since irradiation induces the growth of clusters.

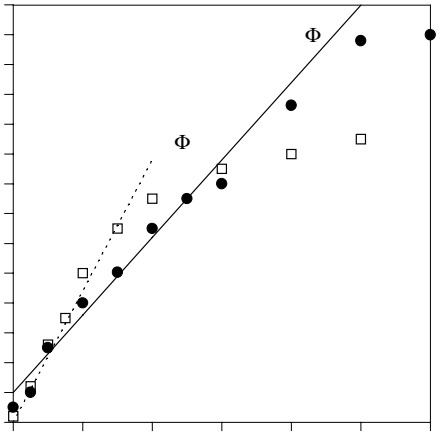

Fig. 4. Variations of the clusters size as a function of the fluence in the sputtered film of Figure 3 (full circles) and in the gel film of Figure 5 (open circles). Linear fits of the growth kinetics are shown with a continuous line for the sputtered film and a dotted line for the gel film.

The adsorption rate of Ag atoms when they reach an interface is certainly instantaneous, taking into account their low solubility in silica and their tendency to precipitate during the films deposition. A "desorption" necessarily occurs since solute Ag atoms are very few at all stages of the irradiation, according to the integral of plasmon resonances. This desorption is an energy-consuming process produced by nuclear collisions and by ionic excitations of atoms located at the interface. It has the effect of dissolving preferentially the smallest clusters in the distribution of sizes, because the desorption rate per unit area of interface is independent of the cluster size and the area/volume ratio varies in inverse proportion to R. Consequently, the found linear kinetics of cluster growth is ascribed to a limitation of the Ag flux between the clusters by the desorption rate. It is also worth to note that radiation-enhanced diffusion in the co-sputtered films can be supposed to occur preferentially along the columns formed during deposition of the film.

According to the fits of peaks, the equilibrium size of clusters at fluences above 10^{15} ions/cm^2 varies only by 60% and their volume by a factor 4 with the Ag concentration in the film, whereas the integral of the plasmon peak is proportional to this concentration. Thus, measurements of optical absorption confirm TEM results: the number density of clusters grows as much as the mean cluster volume in the considered range of concentrations. The equilibrium size is found to be equal to the mean size obtained by annealing a film of same concentration for 1 h at 750 °C (double of that in a film annealed at 500 °C and half of that in a film annealed at 900 °C). The fluctuations of cluster sizes in annealed films should however be controlled by TEM.

For all the studied concentrations, the peaks recorded from as-deposited films or films irradiated with fluences up to 10^{14} appear shifted towards higher energies with respect to Mie resonances of equal width (*i.e.* equal radius R) in silica. Such an effect could be due to several factors:

(a) a refractive index of the matrix lower than 1.475;
(b) a strained lattice of the metal inducing a modification of $\omega_{\rm p}$ and $V_{\rm F}$ in formula (3) [9,10];
(c) a non spherical shape of the clusters.

Vapor deposited films often exhibit a nanoporosity, modifying the refractive index according to the formula:

$$(n_{\rm p}^2 - 1)/(n^2 - 1) = 1 - p,$$

where $n_{\rm p}$ is the index of the porous films, n that of the fully dense material and p the porosity (in volumic %). However, the refractive index of pure silica films deposited with the presently used equipment is exactly equal to 1.475, as established by spectroscopic ellipsometry measurements. Simulations have been performed, varying the parameter β (and keeping the value of K equal to zero, since no interaction effect was expected) and good fits were obtained for β values decreasing from 0.45 to 0.35 with the increasing fluence (see Fig. 3b). According to other theoretical expressions of the polarization for spheroidal clusters [3, 13,14], these values for β would imply that some of the clusters are elongated parallel to the columns observed in TEM and acquire a more stable spherical shape under irradiation. This hypothesis seems more plausible than a decrease of the compression of the metal lattice, since this compression is generally correlated to the surface curvature of the clusters and the cluster size varies little in the sputtered films for the range of fluences where the resonance energy differs from values obtained with the Mie model.

3.2 Gel films

Ag precipitates in siloxane gels derived from TEOS and other Si-alkoxides at room temperature under the effect of day light, at a rate increasing with the Ag concentration [6,15]. The aim of irradiation or heat treatments is twice:

(i) to cross-link the polymeric structure and evolve hydrogen in order to form a chemically resistant oxide;
(ii) to promote a faster growth of the clusters and stabilize their size.

The depletion in H and compaction of the gel network under 4.5 MeV Au irradiation is completed for a fluence of 2×10^{14} cm^{-2} and the gel is converted into pure silica [16].

The distributions of cluster sizes found by TEM are relatively narrow, especially with respect to those reported for similar films subjected to heat treatments (ranging from 5 to 50 nm in films annealed at 500 °C) [15]. Clusters with a mean size of 0.5 nm and a size straggling of 0.3 nm are observed in as-deposited films with Ag concentrations below 2 at.%. Figure 5 shows that the size reached at saturation of the irradiation effect in a film containing 0.3 at.%

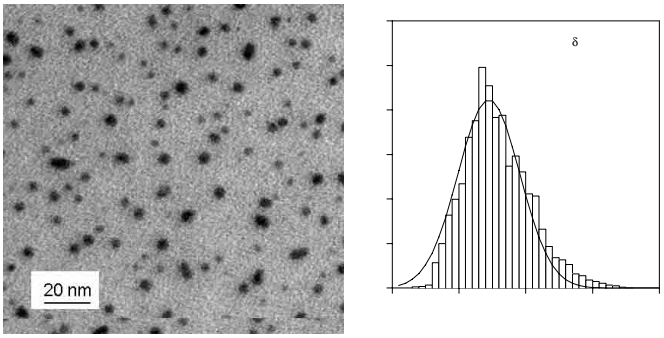

Fig. 5. TEM image of a silica-gel film containing 0.3 at.% Ag (molar ratio 1%), after irradiation with 1.5×10^{15} Au ions and histogram of cluster sizes. The mean radius $\langle R \rangle$ and straggling in the distribution δR indicated in the figure are those found with a Gaussian fit of the histogram (continuous line).

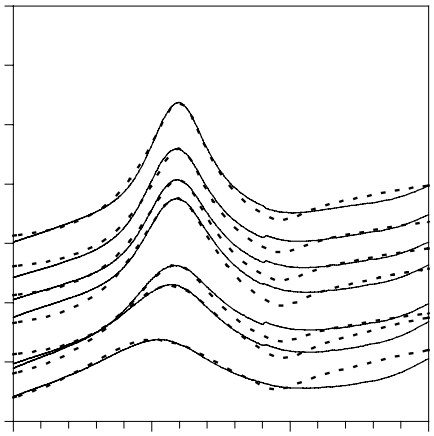

Fig. 6. Optical density of Ag clusters in the same gel film than in Figure 5, after irradiation with fluences indicated in the figure in multiples of 10^{14} ions/cm^2. The Mie simulations fitting spectra are shown with dotted lines. The spectra are shifted vertically for the sake of clarity.

Ag is 1.45 ± 0.45 nm and the clusters seem to be spherical. The mean size and number density of clusters vary with the Ag concentration like in co-sputtered films but clusters are bigger in silica gel films at same concentration and fluence.

Optical absorption spectra from sol-gel films differ from those of sputtered, ion implanted or ion beam mixed films by a noticeable background of absorption, related to defects in the pristine siloxane structure as well as in the glassy product of irradiation. These defects are of different natures, the most important being oxygen deficient centres exhibiting an absorption peak around 5.1 eV [17] and carbon clusters formed from residual ethoxy-groups [16,18]. The absorption by silica defects must be subtracted from spectra because it affects the fitting of the Ag plasmon resonance. For simplifying the correction procedure, the tail of matrix absorption below 4 eV was presumed to be a linear function of the energy and the slope was varied to enable fitting of both the Ag plasmon peak and the magnitude of interband transitions in the Ag clusters by the Mie or effective medium models. A more complex mathematical expression of the matrix absorption would not be very useful, as we do not expect to simulate perfectly the interband transitions by using formula (3) in the case of clusters with quantum sizes. The used procedure reliably removes the undesired background on both sides of the plasmon peak if the residual absorption levels around 2 and 4 eV are consistent with the height of the plasmon peak. The cluster size and volume fraction derived from fits are therefore less questionable than those obtained by TEM observations of this type of films, when they are not fully stabilized by irradiation at high fluences and chemical reactions with solvents used in the preparation of TEM specimens liable to occur, as also a growth of clusters under electron irradiation.

In the optical absorption spectra corrected for the matrix absorption shown in Figure 6 a progressive narrowing of the resonance peak is observed with the increasing ion fluence, indicating that the mean cluster size increases. However, the volume of metallic phase remains almost constant since the integral of the peak varies little for fluences above 10^{14} ions/cm^2. The position of the maximum shifts towards larger energies up to the fluence of 10^{14}, remaining at 3.1 eV for larger fluences.

The interaction between clusters can be neglected since the filling factor is very low. The observed shift of the mean energy of the resonance at low fluences is in perfect agreement with Mie calculations for very small sizes (contrary to the case of co-sputtered films), as shown in Figure 6, and there is no reason to vary other parameters than the cluster size in the fitting procedure. The uniform size deduced from the fits compares fairly well to the mean size of clusters observed by TEM when images are available and Mie calculations permit to assess more precisely minute changes in this mean size with the irradiation fluence than TEM. According to the calculations the mean cluster size increases more or less in proportion to the fluence then it stagnates for fluences higher than 5×10^{14} Au ions/cm^2 (Fig. 4). Thus the growth process seems to be the same than in co-sputtered films.

3.3 Ion implanted silica

Figure 7 shows TEM micrographs of silica implanted with the lowest (a) and highest (b) Ag fluences. It is observed that clusters are already formed for a fluence of 10^{16} ions/cm^2 and their size is relatively uniform, with a mean value of 1.4 nm and a standard deviation of 0.5 nm. For the fluence of 10^{17} ions/cm^2, the frequency of clusters decreases monotonously with increasing size, ranging from 2 to 20 nm. The equivalent size of clusters found by averaging their volumes is 9 nm whereas the mean size obtained by averaging the radii is 6 nm. Equivalent sizes for the fluences of 2×10^{16} and 5×10^{16} atoms/cm^2 should be around 2–3 and 4–5 nm, respectively, assuming that the size increases approximately as the Ag concentration.

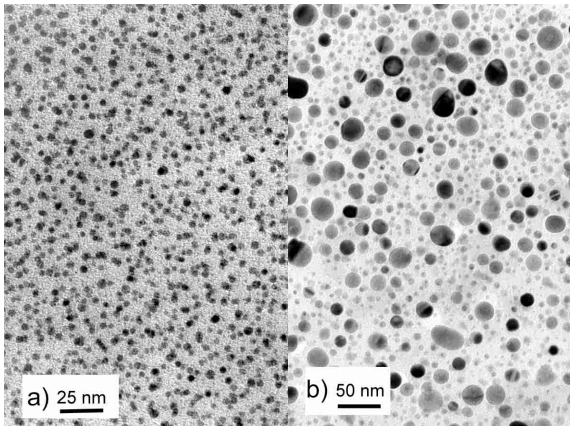

Fig. 7. TEM images of silica samples implanted with (a) 10^{16} and (b) 10^{17} Ag /cm^2 (plane sections).

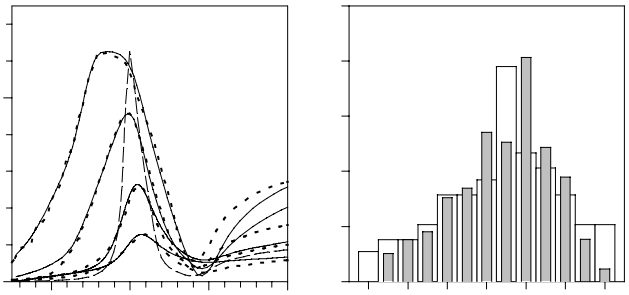

Fig. 8. Spectra of optical density (continuous lines) recorded from silica samples implanted with 150 keV Ag ions at fluences indicated in the figure (unit 10^{16} ions /cm^2). The resonance recorded for the fluence of 10^{17} Ag ions is compared to calculations using the model of effective medium with (dashed line) $f = 30\%$, $R = 9$ nm, $\beta = 1/3$ and $K = 0$, (dotted line) the same values of f, R, β and the distribution of K values filled in grey in (b). The resonance in the specimen implanted with 5×10^{16} Ag has been fitted with (dotted line) $f = 15\%$, $R = 5$ nm, $\beta = 1/3$ and the K distribution filled in white in (b). Spectra of samples implanted with 10^{16} and 2×10^{16} Ag/cm^2 have been fitted (dotted lines) using Mie calculations with cluster sizes of 1.0 and 1.35 nm respectively.

Optical absorption spectra from ion implanted samples with 150 keV Ag ions are presented in Figure 8a. As it can be observed, increasing the ion fluence induces a widening of the peak and a shift towards lower energies for ion fluences over 2×10^{16} cm^{-2}, although an increase of the cluster size in the range of 2 to 20 nm should induce a narrowing of the resonance peak and no significant change of its position. The shape of clusters does not deviate significantly from sphericity. Taking into account that the filling factor f is almost equal to the Ag concentration, since Ag precipitates are already observed for the lowest fluence, and that f reaches 28% for the highest fluence, an interaction between clusters is very probable. In fact, increasing f above 10% in calculations based on the model of effective medium results in a red shift of the resonance and the appearance of a tail on its high energy side.

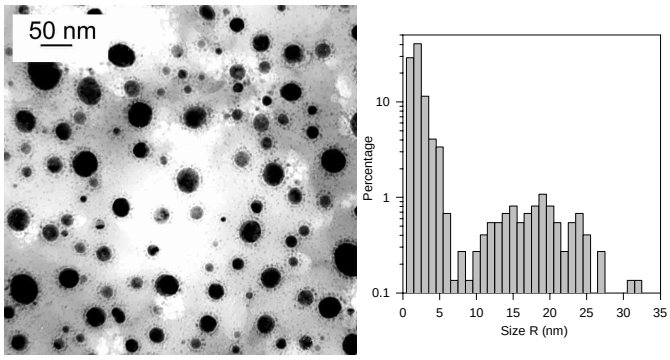

Fig. 9. TEM image of a SiO_2/Ag 8 nm/SiO_2 film ion beam mixed with 1.6×10^{16} Au ions (plane section) and histogram of cluster sizes deduced from measurements on 20 images.

Absorption spectra of samples implanted with the low fluences of 10^{16} and 2×10^{16} Ag could be fitted with plasmon resonances of isolated clusters with spherical shape, assuming uniform sizes of 1.0 and 1.35 nm respectively (Fig. 8a). However, these sizes are smaller than that directly obtained from TEM measurements for the fluence of 10^{16}, or the expected size for the fluence of 2×10^{16}. Contrary to the case of sputtered and gel films, the size distribution, correlated to the Gaussian profile of Ag concentration, could induce a widening of the resonance because of its extent. But the effect of the interaction between clusters could also be already significant for the fluence of 2×10^{16}.

Simulations have been performed with filling factors of 15% and 28%, corresponding to the measured Ag concentrations at the mean range of ions for the fluences of 5×10^{16} and 10^{17} Ag/cm^2, assuming that the clusters are spherical and that their spatial arrangement has no effect on their polarization (factors $\beta = 1/3, K = 0$). The obtained resonances are much narrower than the recorded peaks, as shown in Figure 8a for the sample implanted with 10^{17} Ag ions. Since the clusters seen in TEM images (Fig. 7b) are big enough for being sure that they are spherical, the broadening of peaks must be attributed to fluctuations of their local arrangement, corresponding in the model to variations of the parameter K. The shape of the K values histogram allowing to fit the peaks (see Fig. 8b) is very similar to that obtained by direct calculation assuming a random dispersion of the clusters, although in the present case, we find that the maximum lies on a positive value instead of zero. Therefore, we conclude that the clusters are arranged such that, on average, they increase the polarization of their neighbours.

3.4 Ion beam mixed layers

At ion fluences above 5×10^{15} ions/cm^2 the large clusters formed by lateral segregation in this type of specimen are well separated and surrounded by a halo of smaller clusters resulting from the mixing process (see Fig. 9). For Ag layers of 1 to 15 nm thickness the large clusters have mean sizes of 2.5 times the layer thickness.

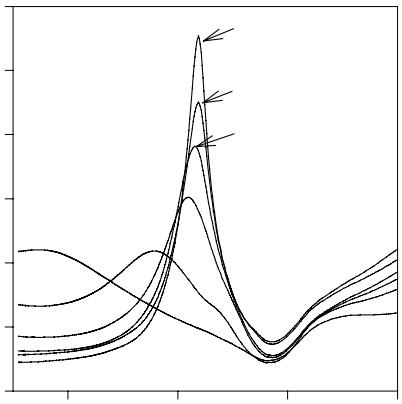

Fig. 10. Spectra of optical absorption recorded from SiO_2/Ag 8 nm/SiO_2 films irradiated with 4.5 MeV Au fluences indicated in the figure in multiples of 10^{15} ions/cm^2.

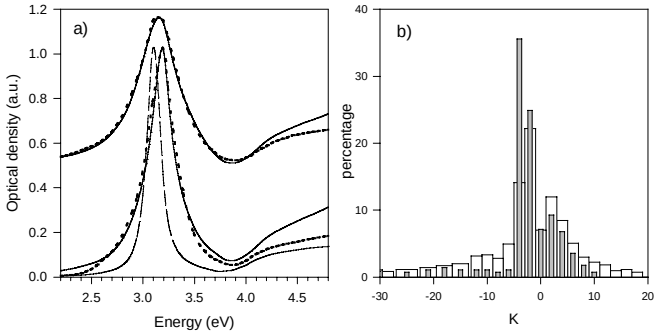

Fig. 11. Comparison of spectra of optical density (continuous lines) recorded from SiO_2/Ag 8 nm/SiO_2 films mixed with 1.6×10^{16} and 6×10^{15} Au ions (shifted by +0.5) to (i) a Mie simulation with the size distribution of Figure 9 (dashed line), (ii) simulations using the model of effective medium (dotted lines) with $f = 30\%$, $R = 20$ nm, $\beta = 1/3$ and the distributions of K values shown in (b). The K distribution filled in grey is related to the film irradiated with 1.6×10^{16} ions.

This size remains constant at fluences in the range 5×10^{15} to 2×10^{16} ions/cm^2 and the number of halo-clusters increases in proportion to the fluence [2].

Figure 10 shows the raw absorption spectra recorded from a 8 nm thick Ag layer embedded in silica, irradiated with incremented fluences of Au ions. The optical resonances in samples irradiated with fluences lower than 5×10^{15} ions/cm^2 will not be analyzed because of the incomplete transformation of the Ag layer into spherical balls. Once this transformation is achieved, the mean energy of the plasmon peak shows no change. As the ion fluence increases, a narrowing of the peak is observed together with an increase in the peak height. This modification of the absorption resonance is ascribed to the precipitation of an increasing number of halo-clusters since the size and shape of the large clusters change very little.

The optical absorption spectra of samples irradiated with fluences above 5×10^{15} ions have been compared to Mie simulations for isolated clusters applying the experimental size distribution determined by TEM and neglecting the decrease of the integral of σ_{ext} for clusters larger than 10 nm. The simulated peak, shown in Figure 11a for a sample irradiated with 1.6×10^{16} ions/cm^2, is much narrower than the experimental one and is situated at lower energy. Clusters with radii smaller than 5nm contribute by less than 5% to the simulated peak. Halo-clusters formed by the mixing process have a maximum size of 2 nm, *i.e.* they do contribute even less. Remarkably, a better fit of the experimental Ag resonance is obtained by assuming that clusters are monodisperse with a size of 2.85 nm while the equivalent size for the Mie calculation, found by weighting volumes by the size histogram, is 8.9 nm. This fact may illustrate how doubtful can be a cluster size estimation by resonance peak analysis, without control by TEM observation.

The width of resonances should remain almost constant for spherical cluster with sizes above about 7 nm, neglecting interaction effects. But the large clusters observed in Figure 9 cannot be considered as isolated. The result of a simulation based on the effective medium model, using a filling factor consistent with RBS results and TEM images ($f = 30\%$), assuming that clusters are spherical and neglecting their arrangement ($\beta = 1/3,\ K = 0$), is shifted to lower energy with respect to the experimental spectrum. Contrary to ion implanted films, the mean value of K in ion beam mixed samples is negative and the distribution becomes narrower with the increasing ion fluence (Fig. 10b). Our interpretation of this effect is that the very small clusters arranged in a spherical halo around each larger cluster act on the local electric field as a uniform charge distribution ρ at the surface of a sphere (depolarization field $E = -(4\pi/3)|\rho|$ [19]).

4 Conclusion

A careful examination of the distribution of cluster sizes and of their spatial arrangement by means of TEM is necessary for interpreting optical properties of metal:insulator colloids. However, after TEM analysis, further information about the clusters may be obtained from the study of optical absorption spectra. When the cluster size distribution is narrow and their filling factor lower than 5%, calculations based on Mie theory can be used to determine their mean size and study their growth under irradiation. This method is particularly useful when the size is not easily measured from TEM images. The analysis of resonances using Mie calculations permitted to establish that the growth of clusters in co-sputtered and gel films is controlled by the rate of dissolution of the smallest clusters.

Clusters formed by ion implantation or ion beam mixing are not big enough to require consideration of the contribution of quadrupole absorption and scattering to their resonance. However, the filling factor and the local arrangement (K parameter in the effective medium model) of the clusters affect the resonance damping. In ion implanted layers this damping increases as the variations of

sizes and distances between clusters with the Ag concentration. On the contrary, the interaction between the large clusters formed by lateral segregation in ion beam mixed layers is screened because of the precipitation of a spherical halo of small clusters.

References

1. P. Mazzoldi, L. Tramontin, A. Boscolo-Boscoletto, G. Battaglin, G.W. Arnold, Nucl. Instrum. Meth. B **80/81**, 1192 (1993)
2. J.C. Pivin, Mater. Sci. Engineer. A **293**, 30 (2000)
3. U. Kriebig, M. Vollmer, *Optical properties of metal clusters* (Springer Series in Material Science **25**, Berlin, Heidelberg, 1996)
4. J.P. Biersack, Nucl. Instrum. Meth. B **27**, 21 (1987)
5. J.A. Thornton, J. Vac. Sci. Technol. **11**, 666 (1974)
6. M. Epifani, C. Giannini, L. Tapfer, L. Vasanelli, J. Am. Ceram. Soc. **83**, 2385 (2000)
7. M.A. Garcia, J. Llopis, S.E. Paje, Chem. Phys. Lett. **315**, 313 (1999)
8. H. Hovel, S. Fritz, A. Hilger, U. Kreibig, Phys. Rev. B **48**, 18178 (1993)
9. W. Cai, H. Hofmeister, M. Dubiel, Eur. Phys. J. D **13**, 245 (2001)
10. J. Lerné, M. Pellarin, E. Cottancin, M. Gaudry, M. Broyer, N. Del Fatti, F. Vallée, C. Voisin, Eur. Phys. J. D **17**, 213 (2001)
11. J. Philibert, *Atom movements diffusion and mass transport in solids* (EDP Sciences, Les Ulis, France, 1991)
12. Z. Wang, Nucl. Instrum. Meth. B **2**, 784 (1984)
13. R.W. Cohen, G.D. Cody, M.D. Coutts, B. Abeles, Phys. Rev. B **8**, 3689 (1973)
14. Galeener, Phys. Rev. **27**, 421 (1971)
15. P. Innocenzi, H. Kosuka, S. Sakka, J. Sol-gel Sci. Technol. **1**, 305 (1994)
16. J.C. Pivin, P. Colombo, G. Soraru, J. Am. Ceram. Soc. **83**, 713 (2000)
17. *Proceedings of the NATO Advanced Institute on Defects in SiO_2 and related dielectrics: Science and technology*, Erice, Italy, 2000, edited by G. Pacchioni, L. Skuja, D.L. Griscom (Kluwer Academic Pub, Dordrecht, 2000)
18. J.C. Pivin, P. Colombo, A. Martucci, G.D. Sorarù, E. Pippel, M. Sendova-Vassileva, *Proceed. Int. Workshop on Glasses, Ceramics and Nanocomposites from Gels*, J. Sol-gel Sci. Technol., to be published
19. C. Kittel, *Introduction to Solid State Physics*, 5th edn. (John Wiley & Sons, Inc., New York, 1976), p. 404